International Journal of Climatology

RMetS Royal Meteorological Society

# Spatio-temporal drought patterns of multiple drought indices based on precipitation and soil moisture: A case study in South Korea

| | |
|---|---|
| Journal: | *International Journal of Climatology* |
| Manuscript ID | JOC-18-0642.R2 |
| Wiley - Manuscript type: | Research Article |
| Date Submitted by the Author: | 03-Apr-2019 |
| Complete List of Authors: | Kwon, Moonhyuk; University of Bristol Department of Civil Engineering, Civil Engineering<br>Kwon, Hyun-Han; Sejong University, Department of Civil and Environmental Engineering<br>Han, Dawei; University of Bristol, Department of Civil Engineering |
| Keywords: | SPI, SSI, Multivariate drought index, Clustering analysis, Quantile regression |
| Country Keywords: | Korea, Republic Of |
| | |

# Spatio-temporal drought patterns of multiple drought indices based on precipitation and soil moisture: A case study in South Korea

*Spatio-temporal drought patterns of multiple drought indices*

Moonhyuk Kwon[1], Hyun-Han Kwon[2, *] and Dawei Han[1]
Civil and Environmental Engineering, University of Bristol, United Kingdom
Department of Civil and Environmental Engineering, Sejong University, Seoul, South Korea
(***Contact:** *hkwon@sejong.ac.kr*)

**Abstract**

This study aims to explore the spatio-temporal characteristics of meteorological and agricultural droughts using the Standardized Precipitation Index (SPI) and Standardized Soil Moisture Index (SSI), respectively, as well as their relationships over the past three decades (1986-2016) in South Korea. The SSI shows less frequent droughts and longer drought duration compared to the SPI, due to the gradual decrease in the autocorrelation functions of the SSI. The strongest cross-correlations are observed at a 1-month lag between the SPI and SSI for most stations. Thus, the SPI could be more appropriate for defining the onset of a drought, whereas the SSI appears to be more effective for describing drought persistence. Moreover, the transition from meteorological to agricultural droughts is significantly dependent on the season, indicating that the transition between them is highly correlated with antecedent moisture conditions. The copula-based Multivariate Standardized Drought Index (MSDI) is introduced to explicitly postulate interdependence between the SPI and SSI in the context of a multivariate probability distribution. We employ a hierarchical agglomerative clustering approach along with a quantile regression model to better understand the spatio-temporal pattern of the MSDI. More drought episodes under moderate to severe drought conditions are observed along the southern coast of South Korea. Additionally, persistent droughts with higher severity are observed in the northern part of South Korea, which may be attributed to a significant decreasing trend (or increasing drought risk).

**Keywords:** SPI, SSI, Multivariate drought index, Clustering analysis, Quantile regression

## 1. Introduction

Drought is a periodic phenomenon that exerts multifaceted negative impacts on a wide range of water-related sectors, which can eventually lead to severe direct (or indirect) socio-economic losses (Mckee et al. 1993; Spinoni et al. 2014; Vidal et al. 2009). Droughts occur virtually everywhere in the world, but their characteristics, such as duration, intensity and

frequency, vary significantly depending on climate zones (Mirabbasi et al. 2013). Additionally, it is expected that climate change will accelerate changes in drought characteristics (Dai 2011; Van Loon et al. 2016). Thus, drought monitoring and early warning systems at global and local scales have emerged as powerful platforms for preventing and mitigating the negative effects of drought.

Drought is rather different from other water related hazards in terms of its spatio-temporal characteristics, resulting in structured spatial coverage with varying durations. Moreover, the spatio-temporal drought patterns may differ substantially by drought intensity. In these contexts, an exploration of the spatio-temporal drought patterns over different quantiles (i.e. severity) can serve as a basis to understand the evolution and nature of droughts in space and time. However, most of existing studies on droughts have not specifically analyzed the spatio-temporal patterns at different quantiles. Thus, this study will focus on exploring the underlying structure of drought occurrence and development.

Many studies have been conducted to estimate the onset, persistence and termination of drought events using meteorological and hydrological variables (Ganguli and Ganguly, 2016; Mo, 2011; Shukla et al., 2011; among others). Drough features such as duration, severity and intensity are commonly characterized by drought indices, which provide a more comprehensive perspective for drought monitoring and management compared to the direct use of hydro-meteorological variables (e.g., precipitation, soil moisture (SM) and streamflow) (Zargar et al. 2011). Nonetheless, the selection of the drought index for a certain purpose remains controversial (Farahmand & AghaKouchak 2015). Specifically, the identification of drought can be attributed to the choice of drought index that, with some limitations, incorporates different aspects of drought conditions (Hao & Singh 2015). Accordingly, various drought indices have been proposed to detect different types of droughts. For example, a meteorological drought index refers to deficits in precipitation and/or evaporation,

whereas agricultural and hydrological drought indices are based on deficits in SM and streamflow, respectively (Dracup et al. 1980).

The drought indices are mainly used to describe different types of droughts (i.e. meteorological, agricultural, hydrological, and socioeconomic droughts). They are commonly derived from a single hydrological variable (e.g., rainfall: the standardized precipitation index (SPI), and standardized anomaly index (SAI), streamflow: standardized streamflow index (SSI) and streamflow drought index (SDI), groundwater: standardized water-level index (SWI) and soil moisture: Standardized soil moisture index (SSI)). On the other hand, there are several examples that combine two or more variables such as the Palmer drought severity index (PDSI; Palmer, 1965), standardized precipitation evapotranspiration index (SPEI; Vicente-Serrano et al., 2010), surface water supply index (SWSI; Shafer and Dezman, 1982) and multivariate standardized drought index (MSDI; Hao and AghaKouchak, 2013). Here, we only introduced some of the drought indices, and would suggest that for more details readers are kindly referred to Svoboda and Fuchs (2017). Among many drought indices, the SPI, proposed by Mckee et al., (1993), has been widely adopted as a tool for monitoring long-term drought conditions at multiple time scales. More specifically, the advantage of the SPI method lies in its relative simplicity of computation and ease of interpretation, and the SPI approach is particularly useful in predicting drought onset (Hao & AghaKouchak 2013). Thus, the World Meteorological Organization (WMO) endorsed the SPI as a standard drought indicator (Hayes et al. 2011). The fundamental idea behind the SPI can be applied to other hydrometeorological variables with the objective of building a standardized drought index (Van Loon 2015; Kumar et al. 2016).

Each drought index has limitations and strengths in measuring drought conditions. For instance, previous studies have shown that the SPI is more likely to detect the emergence of drought conditions, whereas drought persistence can be more effectively identified based on

the SM deficit (Mo 2011). In other words, drought information based on a single index may not be sufficient to provide an integrated picture of different types of drought (Kao & Govindaraju 2010). This issue has, in turn, led to the need for a combination of multiple drought indices that are derived from different hydrologic variables including rainfall, SM, groundwater and streamflow. Such hydrological variables particularly have been used to construct a joint drought index to characterize the complex nature of drought (Mirabbasi et al. 2012; Hao & Singh 2015).

Considering that drought is a multidimensional phenomenon, combining multiple variables (e.g., from precipitation to SM) is beneficial for successful drought preparedness and mitigation, and particularly useful for communication purposes between different types of drought. Here, we adopt the MSDI proposed by Hao and AghaKouchak (2013) that can combine meteorological and agricultural droughts, and the composite drought index was then grouped by the hierarchical agglomerative clustering approach for classifying regional patterns. Over the past decade, many researchers have proposed statistical models to build a multivariate drought index. In the context of multivariate analysis, copulas have been used in a wide range of hydrological studies such as multivariate drought frequency analysis (e.g., Ekanayake and Perera, 2014; Kao and Govindaraju, 2010; Kwon *et al.*, among others), flood frequency/risk analysis (e.g., Favre *et al.*, 2004; Jongman *et al.*, 2014; Zhang and Singh, 2006), and rainfall simulation (Li et al. 2013). In this study, because of the interdependence and interaction between rainfall and SM, the copula-based MSDI (Hao and AghaKouchak, 2013) is used to consider the two indices (i.e., the SPI and SSI) jointly in the context of a multivariate probability distribution.

A key aim of this study is to explore a spatio-temporal drought pattern on the regional scale. A number of previous studies have been carried out to investigate regional drought patterns using cluster analysis, principal component analysis (PCA) or a combination of the two

techniques. Among them, clustering analysis, also known as an unsupervised classification model, is widely used to classify drought patterns into certain categories according to their relationships; such analysis can identify specific spatio-temporal patterns within the cluster (Shamshirband et al. 2015). Santos et al. (2010) employed K-means clustering and PCA to assess spatial and temporal patterns of the SPI series, whereas Yoo et al. (2012) applied the K-means approach to partition their study region into several sub-regions based on bivariate drought attributes. Furthermore, spatio-temporal drought patterns were regionally summarized by combining a quantile regression model and hierarchical agglomerative clustering algorithm (Shiau & Lin 2016; Yang et al. 2017). Despite the above-mentioned potential uncertainty in identifying drought features using a drought index based on a single variable, clustering analysis has not been applied extensively for a multivariate drought index. In other words, most studies on clustering analysis were dedicated to the delineation of homogeneous regions using a single drought index or their drought characteristics (e.g., duration, severity, and frequency).

Moreover, given that the nonstationarity in drought episodes is of increasing concern, the nonparametric Mann-Kendall (MK) test has been widely used to identify significant changes in drought pattern (Subash & Ram Mohan 2011; Güner Bacanli 2017). Despite its popularity in the hydrological community, the MK approach cannot be applied to explore the temporal variability of hydrologic variables at various quantiles of the distribution (Shiau & Lin 2016), which is important for water resources management, especially for extreme rainfall that translates into both droughts and floods. In this regard, this study uses a quantile regression model proposed by Koenker and Bassett (1978) to explore the non-Gaussian distribution of trend in drought characteristics in terms of the predefined quantiles (e.g., moderate, severe and extreme drought).

The main contributions of this study are threefold: (1) we propose to use a global reanalysis SM dataset to derive the SSI drought indices and its use to explore the transition from meteorological to agricultural droughts; (2) we propose quantile regression model-based spatio-temporal drought analysis at different quantiles, and (3) we classify spatio-temporal drought patterns using the multivariate drought index and the hierarchical agglomerative clustering approach, covering the period 1986-2016 across South Korea.

A brief background of this study was presented in this section. In the following section, we illustrate the precipitation and SM data and further describe the drought indices considered in this study. The theoretical aspects of modeling approaches including quantile regression, copula function and clustering analysis are provided in Section 3. The spatio-temporal analysis of the drought indices over South Korea obtained from this study is illustrated in Section 4, followed by conclusions and future tasks in Section 5.

## 2. Hydrologic Data and Drought Indices

### 2.1. Precipitation and Soil Moisture Data

The historical daily precipitation data measured at 55 weather stations over South Korea, which are operated by Korea Meteorological Administration (https://web.kma.go.kr/eng/), are collected for the period 1986-2016. Figure 1 shows the locations of weather stations used in this study. Additionally, a global SM data set from the European Centre for Medium-Range Weather Forecasts (ECMWF) are used. ECMWF releases global reanalysis SM datasets (i.e. ERA-Interim) daily in quasi-real time with high spatial resolution, in 6-hour intervals, at four depths (i.e., 0-7, 7-28, 28-100 and 100-289 cm) (Albergel et al. 2012). ERA-Interim reanalysis data provides a spatial resolution of approximately 25 km covering the period 1979-present and can be accessed from *https://www.ecmwf.int/*. The accuracy of the ERA-Interim reanalysis data was assessed against in-situ observations from 117 stations across the

159 world by Albergel et al. (2012). Their results revealed robustness for various climate
160 conditions with a reasonable level of accuracy; similar results were also achieved based on
161 our preliminary analysis in the study area (see Figure S1). The Pearson correlation
162 coefficients between the original ERA-Interim and the currently available in-situ SM data
163 over all of South Korea are reasonably high, ranging from 0.60 to 0.75.
164 In our study, SM data are collected at 6-hour intervals (0:00, 6:00, 12:00 and 18:00 UTC)
165 from the locations with centroids nearest to the weather stations and averaged to obtain a
166 daily mean SM time series. The root-zone SM has a significant impact on crop yield so that it
167 is evident that crop growth and root development should take into consideration in designing
168 agricultural drought indices (Narasimhan & Srinivasan 2005). In this respect, the ERA-
169 Interim SM data at the third layer (28-100 cm) are mainly used as the best proxy of the root-
170 zone SM in this study. Both rainfall and SM data are then accumulated on a monthly basis for
171 subsequent study.
172 **[Fig. 1; Tab. 1]**
173

174 **2.2. SPI and SSI Drought Indices**

175 The SPI has been widely used to effectively measure and detect the extent of a deficit of
176 precipitation, providing locally specific early warnings of drought (Clayton 1978). Its
177 popularity stems from its flexibility and ease of use for detecting droughts at multiple time
178 scales (Ganguli & Ganguly 2016). Since the SPI was designed to provide a dimensionless
179 index, SPI values can often be used to spatio-temporally compare an overall view of the
180 drought at a national or global scale for a range of practical applications (Djerbouai & Souag-
181 Gamane 2016). To compute the SPI, daily precipitation data is first aggregated at different
182 timescales (e.g., 3, 6, 12, 24 or 36 months). In this study, we primarily focus on the SPI at 3-
183 and 6-month timescales (hereinafter, SPI-3/6) to investigate the characteristics of

meteorological droughts and their spatio-temporal patterns. The aggregated precipitation data are typically fitted to theoretical distribution functions such as the gamma and Pearson type III distributions (Farahmand & AghaKouchak 2015). The SPI is then computed by transforming the cumulative probability distribution into standardized normal variates with zero mean and standard deviation equal to one (Mckee et al. 1993; Guttman 1999). However, because the optimal probability distribution of rainfall can vary substantially, a parametric approach is less flexible, leading to inconsistent results (Vidal et al. 2009; Kumar et al. 2016; Farahmand & AghaKouchak 2015). In other words, the SPI values are inherently susceptible to the selection of a distribution function. Therefore, we employ a non-parametric kernel density estimation approach to reduce the sampling error associated with the choice of distribution functions. While the SPI is mainly used to identify meteorological drought, agricultural drought is generally represented by the SM deficit. Accordingly, the SSI, known as an agricultural drought index monitoring the extent and degree of SM, plays a complementary role in a comprehensive review of drought conditions. Similarly, the kernel density estimation approach was used to transform SM data into the SSI. In this study, we extracted information on the durations and severities (i.e., deficit volumes) from SPI and SSI time series. Drought duration refers to the periods of the continuously negative phase, whereas drought severity is the sum of cumulative deficits over the corresponding duration (Kwon et al., 2016). Table 2 shows the SPI drought criteria defined by Mckee et al. (1993). Note that the same drought severity categories are subsequently applied to the SSI and MSDI.

**[Tab. 2]**

## 3. Methodology

### 3.1. Quantile Regression

208 This study aims to assess not only the overall trends of drought characteristics but also the
209 non-Gaussian distribution of trends in drought duration, severity and frequency at various
210 levels of quantiles. The first-order quantile regression (Koenker and Bassett, 1978) is applied
211 to identify temporal trends in different drought characteristics. The $\tau^{th}$ quantile regression
212 estimate is computed by minimizing Equation 1 as follows:

213 $$min\sum_{i\,:y_i \geq\ \alpha_\tau+\beta_\tau x_i}\tau|y_i-\alpha_\tau-\beta_\tau x_i|+\sum_{i:\,y_i <\ \alpha_\tau+\beta_\tau x_i}(1-\tau)|y_i-\alpha_\tau-\beta_\tau x_i| \qquad (1)$$

214 …where $\alpha_\tau$ and $\beta_\tau$ are regression coefficients associated with the quantile $\tau$, ranging between
215 0 and 1, and $y$ indicates the drought indices (i.e., the SPI and SSI). In this study, the null
216 hypothesis of a zero slope for drought characteristics was tested at a level of 95% at quantile
217 $\tau$.
218
219 **3.2. Overview of the Copula Function**
220 In order to better represent the interdependence between precipitation and SM, we used the
221 MSDI based on the joint distribution of two drought indices (i.e., the SPI and SSI). Among
222 various types of multivariate models, the copula has been widely applied in various areas
223 including hydrological and climatological applications since the copula can effectively link
224 the marginal distributions together to construct the joint distribution (Kwon et al. 2016; Kao
225 & Govindaraju 2010; Favre et al. 2004). From a modeling viewpoint, Sklar's Theorem (Sklar
226 1959) allows us to model the marginal distributions separately from the dependence structure,
227 which is described by a copula parameter $C$ (Rüschendorf 2009; Lall et al. 2016; Requena et
228 al. 2013; Salvadori & De Michele 2004). The proposed approach provides a useful
229 framework to assess overall drought conditions since the MSDI can integrate different
230 aspects of drought dynamics, covering meteorological and agricultural droughts. Here, we
231 briefly introduce the concept of the copula. For more details, readers are kindly referred to
232 Joe (1997); Nelsen (1999); and Salvadori and De Michele (2004). Let the SPI and the SSI be

continuous random variables $X$ and $Y$. If a joint distribution exists with the marginal distribution $F(X)$ and $G(Y)$, then the cumulative joint probability $p$ with a copula $C$ can be represented as Eq. (2):

$$P(X \leq x, Y \leq y) = C[F(X), G(Y)] = p \quad (2)$$

Finally, the cumulative joint probability $(p)$ of the SPI and SSI can be transformed into the MSDI as follows (Hao & AghaKouchak 2013)…

$$\text{MSDI} = \varphi^{-}(p) \quad (3)$$

…where $\varphi^{-}$ is the inverse of the standard normal distribution function. The parameters of the copula functions are estimated using the maximum likelihood (ML) method, and the optimal copula for drought variables (i.e., $X$ and $Y$) is then selected based on the Akaike Information Criteria (AIC) (Akaike 1974). In this study, an optimal copula for each station is selected from five copula functions (i.e., Gaussian, t, Clayton, Frank and Gumbel). More details are found in Li et al., (2013) and Clayton, (2016).

### 3.3. Clustering Analysis

The hierarchical agglomerative clustering analysis is adopted to classify spatio-temporal drought patterns into certain categories, which is carried out in the MATLAB environment. The algorithm, application and implementation of this technique can be found in the literature (Martinez & Martinez 2004). In this manner, weather stations are partitioned into subsets by defining a measure of distance or dissimilarity in terms of drought features. In other words, each category should be mutually exclusive, and the drought characteristics assigned to a certain category should be as similar as possible. The hierarchical agglomerative clustering approach begins with a measure of the similarity (or dissimilarity) between the objects (i.e. the MSDI time series over 55 weather stations) that are initially regarded as an individual cluster, and the individual clusters are then successively merged until one cluster includes all

objects. In this study, Ward's method, which is referred to as an increase of sum-of-squares, is used to assess the proximity between two clusters…

$$(r, s) = \sqrt{\frac{2n_r n_s}{(n_r + n_s)}}\ ||\bar{x}_r - \bar{x}_s||_2 \qquad (4)$$

…where $||\ ||_2$ is the Euclidean distance, $\bar{x}_r$ and $\bar{x}_s$ are the centroids of clusters $r$ and $s$, and $n_r$ and $n_s$ are the number of elements in clusters $r$ and $s$.

## 4. Results and Discussion

### 4.1. Drought identification and Relationship between the SPI and SSI

To explore drought propagation, we first evaluate cross-correlations between the SPI and SSI to quantify the lag time over the entire array of weather stations for 3- and 6-month accumulation periods, as shown in Figure 2 (Samples of cross-correlation between the SPI-n and SSI-n can be seen in Figure 3). Here, the strongest cross-correlation at each station is marked by a black dot. In other words, it appears to take one month at most weather stations (i.e., 50 stations for 3-month and 48 stations for 6-month accumulation periods out of 55 weather stations, respectively) for precipitation deficits to propagate to SM deficits through the hydrological cycle. In addition to the above drought features, an understanding of drought persistence, which has an impact on water resources management, is also of great interest for hydrologists (Meng et al. 2017; Ganguli & Ganguly 2016; AghaKouchak 2015). Drought persistence can be computed by the length of a dry spell for a certain threshold or by using temporal autocorrelations (Tatli 2015).

**[Figs. 2-3]**

We further explore a monthly variation of the correlation coefficient between the SPI-3 and SSI-3 for the 55 weather stations, and the lagged relationships between the drought indices are additionally examined to capture any possible delayed response. As shown in Figure 4, the SPI is in general positively correlated with the SSI, thus confirming that the deficit of SM

283 is substantially related to the meteorological drought (Van Loon 2015). However, there exist
284 seasonal variations in correlation coefficients, which can be explained by the fact that
285 agricultural drought in response to the deficit in rainfall may differ significantly, depending
286 on the season. Furthermore, it can be concluded that the stronger relationship begins when
287 rainfall starts after a long, dry winter-spring season in South Korea. In this stage, the water
288 moves both through the soil and over the surface via a range of hydrologic processes such as
289 base flow, seepage, infiltration and runoff throughout the summer. In contrast, the
290 relationship weakens as SM content decreases below the wilting point, with the relationship
291 continuing to weaken until the next wet season. Interestingly, it appears that during a dry
292 season (winter-spring), there is a more robust relationship between the SPI and the 1-month
293 lagged SSI. It can be concluded that the SSI has a delayed response to the SPI under dry soil
294 conditions, whereas for wet soil conditions, the prompt response of the SSI to the SPI is
295 dominant. In this perspective, it is acknowledged that the characteristics of the transition from
296 meteorological drought to agricultural drought are significantly dependent on antecedent SM
297 content over the season. Thus, we should consider the issue of presenting the role of
298 antecedent SM content in connection with evidence concerning changes in the drought
299 propagation feature over time.

300 **[Fig. 4]**

301 We investigate the temporal persistence of the drought indices using the autocorrelation
302 function representing drought persistence over the entire array of weather stations. As shown
303 in Figure 5, it is evident that the autocorrelation functions of SSI decrease gradually with
304 higher degrees of autocorrelation compared to that of the SPI for both accumulation periods.
305 On the other hand, the results also highlight the potential benefit of using different drought
306 indices, i.e., the onset of a drought condition can be detected by the meteorological index
307 (i.e., the SPI) earlier, whereas the SSI seems to be more appropriate for reliably describing

308 drought persistence (Farahmand & AghaKouchak 2015; Entekhabi et al. 1996). In this
309 regard, we introduced a robust framework that allows multiple drought indices to be
310 combined. The results associated with the combined drought indices are presented in Section
311 4.3.

312 **[Fig. 5]**

313

314 **4.2. Spatial Pattern of Drought over South Korea**

315 For each accumulation period (3- and 6- month), drought events are identified using a
316 threshold of -1.0 and their spatial distributions along with durations are displayed in Figure 6.
317 The cokriging method (Pebesma 2004) is hereinafter employed to obtain the regional
318 distribution of drought characteristics. Compared to the SPI, the SSI shows less frequent
319 droughts for both accumulation periods, which can be attributed to the stronger persistence
320 (i.e., a smaller fluctuation) that is more likely to be characterized by the SSI (Farahmand &
321 AghaKouchak 2015). Furthermore, more frequent drought events appear to occur at a shorter
322 timescale for both drought indices (Figures 6c and g), due to the relatively weaker persistence
323 (Figures 6d and h). It was also clearly seen that drought duration of the SSI is significantly
324 longer than that of the SPI, and the difference becomes more distinct for a longer timescale.
325 In other words, the 3-month drought indices pertain negative values more frequently than do
326 the 6-month drought indices, and the SPI recovers to wet states more quickly than does the
327 SSI. More frequent drought events with the threshold -1.0 particularly stand out in western
328 central South Korea for the SPI, while an increased frequency of moderate droughts is
329 identified in the southern and northern parts of South Korea.

330 **[Fig. 6]**

331 Next, drought characteristics such as duration and severity for the SPI and SSI are extracted
332 and their spatial distributions are presented in Figures 7 and 8. For SPI-3, a longer drought

duration is predominantly identified in the northern and southern parts of South Korea and the magnitude of drought severity is found to be similar to the spatial distribution of drought duration. Yet, as the accumulation period increases (i.e., SPI-6), the spatial extent of droughts is partially extended to the east coast. As expected, for both drought accumulation periods, the spatial distribution of drought over South Korea clearly reveals the strong spatial coherence between drought duration and severity. That is, regions with a prolonged drought tend to experience more severe droughts, leading to more severe effects on water resource management and vice versa. Additionally, there is a tendency for duration and severity to increase in proportion to the accumulation period for either SPI or SSI. As shown in Figures 7-8, there are some differences in the spatial distribution of duration and severity between the SSI and SPI. It can be seen that the SSI consistently yields higher drought durations and severities, compared with the SPI. Again, this may be attributed to the stronger persistence of the SSI. Locally significant severe droughts in terms of both drought duration and severity are primarily represented in the southeastern region. Interestingly, the spatial distribution of drought characteristics associated with the SPI is more dependent on the accumulation periods (see Figure 7), while the SSI is less sensitive to the accumulation periods (see Figure 8).

**[Figs. 7-8]**

The entire time series of the SPI-6 and SSI-6 were divided into two halves (i.e. 1st period (1987-2001) and 2nd period (2002-2016)), and the drought events and their durations and severities were extracted using a threshold of -1.5. Note that the values given here are the average values over the entire weather stations during that period. For the SPI-6 (Figures 9a-c), the number of drought events are significantly decreased in the second half, while the duration and severity are slightly increased. It can be concluded that the decreasing trend in the drought events is apparently due to an increasing trend in precipitation since the SPI

represents deficits in precipitation. Relative to the decreasing trend in the number of drought events, a severe and prolonged drought has been observed over the last decade due to a recent increase in interannual climate variability (Nam et al. 2015). On the other hand, for the SSI-6 (Figures 9d-f), a drought with more pronounced frequency and severity compared to the SPI-6 was found in the second half. It may be the consequence of a significant increasing trend in temperature during the recent period while the recent decrease in precipitation may play a limited role for the tendency toward increased drought frequency and severity.

**[Fig. 9]**

The trends in the SPI and SSI time series covering 1986-2016 are further analyzed using a quantile regression model. The estimated slope parameters for the predefined drought categories (Table 2) at 55 weather stations are spatially interpolated. As shown in Figures 10a and d, for both indices, the trends for moderate drought (i.e., threshold -1.0) showed a downward tendency in the northern part of South Korea, while an upward trend is dominantly localized in the southern region. Interestingly, there exist significant differences in the spatial presence of trends in extreme drought (i.e., threshold -2.0) between the SPI and SSI. More specifically, the SSI shows a decreasing tendency over the entire region, while there is no significant difference in the spatial distribution of drought trend over different drought states for the SPI. In summary, there appears to be a more pronounced decreasing tendency (or increasing risk) of the drought in the northern part of South Korea. In South Korea, nearly 50-60% of total annual rainfall occurs during the summer monsoon season (Kim et al. 2002). It has been reported that a general declining trend is evident in the East Asian summer monsoon, and this tendency appears to be more prevalent since the early 1990s (Li et al. 2017). Similarly, the increased drought risk in the northern part of South Korea may be linked to weakened summer monsoons over the last three decades, which can be associated

382 with stagnation of the monsoon activity in the middle of South Korea, and then retreat toward
383 a lower latitude (Zhang & Zhou 2015).

384 **[Fig. 10]**

385

386 **4.3. Clustering Analysis on Multivariate Standardized Drought Index (MSDI)**

387 A hierarchical clustering approach is applied to explore regional trends in droughts over the
388 last three decades. One may consider a direct use of two drought indices for clustering
389 regional patterns. However, based on our preliminary analysis (see Figures S3-S4), the
390 distribution of the identified clusters in the SPI and SSI are significantly different, thus
391 confirming that the direct use of indices together for the clustering may fail to identify
392 regional patterns of drought. On the other hand, with multi-dimensional data, one can employ
393 multivariate techniques, such as copulas, which can provide a better estimation for
394 dependencies among the variables, prior to clustering. Specifically, we introduce the MSDI to
395 provide a comprehensive perspective of the drought by constructing a joint probability
396 distribution between the SPI and SSI. We consider two types of elliptical copulas and three
397 types of Archimedean copulas to model the dependency structure of the drought indices,
398 namely the student t, Gaussian, Clayton, Frank and Gumbel. As discussed in the
399 methodology section, the marginal distributions are first specified with the independent
400 identically distributed (IID) assumption for the drought variables, and the interdependence
401 between the variables is then described through the copula functions. In this study, it might
402 be desirable to assume the Gaussian distribution for the marginal distributions for both the
403 SSI and SPI, since the indices are already normalized to their respective values. A set of
404 parameters for the MSDI, four parameters in the marginal distribution and one parameter in
405 the copula function, are estimated by using the maximum likelihood method (Kao &
406 Govindaraju 2010; Renard & Lang 2007; Bouyé et al. 2000), and the optimal copula

functions are then selected using the Akaike Information Criteria (AIC) for each weather station. Among five types of copulas, the Frank copula is generally selected for both accumulation periods, and the spatial distribution of the selected copula is presented in Figure S5.

We use clustering analysis to explore the presence of a regional trend in drought, and an important issue with respect to the clustering approach is to determine the number of desired clusters. To systematically choose the optimum number of clusters with the hierarchical agglomerative clustering algorithm, the algorithm is recursively applied to the MSDI series with an increasing number of clusters and the optimum number of clusters is selected by maximizing (or minimizing) some measure of fitness. This study uses the upper-tail rule, proposed by Mojena (1977), as a measure of model fitness. The best cut-off level (i.e., the number of clusters) is determined by the distance analysis of the standardized fusion levels in a dendrogram. As shown in Figure 11, the inflection points of the MSDI-3 is found at a cut-off level of four (Figure 11a). In other words, the degree of decrease in the standardized fusion level is negligible for more than four clusters. On the other hand, an inflection point is found at five clusters for the MSDI-6 (Figure 11b). Therefore, four clusters for the MSDI-3 and five clusters for the MSDI-6 are subsequently selected for further analyses.

**[Fig. 11]**

The distribution of the resulting clusters is contiguous rather than spatially separated for both accumulation periods, as presented in Figure 12. It can be concluded that the results are more physically interpretable, which can lead to more effective strategies in the development and implementation of drought management and mitigation plans for certain areas. There is a notable contrast to the clustering over accumulation periods in the northern part of South Korea, namely Gyeonggi province and Gangwon province. More specifically, two subcategories, representing Gyeonggi and Gangwon province, in MSDI-6 are grouped

together as a category in MSDI-3. For a given cluster, this study further explores different aspects of drought features such as duration, severity and long-term trends at different quantile levels.

**[Fig. 12]**

The spatially averaged MSDI values over each cluster are shown in Figures 12-13, and their trends appear to differ significantly between thresholds (or exceedance probabilities; moderate (-1.0): 0.16, severe (-1.5): 0.07 and extreme (-2.0): 0.02). Compared to the MSDI-6, more frequent drought events appear to be identified at the MSDI-3, and the number of drought events for certain drought categories varies over different clusters, as summarized in Table 3. It is evident that drought duration of the MSDI-6 is significantly longer than that of the MSDI-3, and the difference becomes more distinct under extreme drought conditions. Similarly, an overall increase in drought severity in the MSDI-6 is clearly observed. Specifically, more moderate to severe drought episodes are observed in the northern part of South Korea, covered by clusters CL-3 and CL-4 for the MSDI-3 and by clusters CL-1 and CL-2 for the MSDI-6. Clusters CL-2 for the MSDI-3 and CL-4 for the MSDI-6 notably for the longer duration period and the higher severity are mainly identified along the southern coast, under moderate to severe drought condition. Spatially aggregated drought features vary under extreme drought conditions. In other words, CL-3 for the MSDI-3 indicates a much more extreme drought condition in the northern part of South Korea, and as does CL-4 for the MSDI-6 in the southern coast.

**[Tab. 3]**

Additionally, we explore regional trends over predefined thresholds using a quantile regression model, as represented in Figures 13-14 and Table 4. Numbers in bold are statistically significant at the 0.05 level ($p < 0.05$) in Table 4. For the MSDI-3, CL-1 representing drought in the central eastern region showed no trend for all four levels, while a

457 significantly decreasing trend is shown in CL-3. A significantly decreasing trend (or
458 increasing drought risk) in MSDI-3 was found at CL-2 (e.g., median) and CL-4 (e.g.,
459 extreme, moderate and median). Overall, for a longer-duration MSDI-6, a significant
460 downward trend becomes more dominant. Furthermore, we explore the past three major
461 drought episodes over the last three decades (1986-2016), as illustrated in Figures 13-14. As
462 presented, drought episodes Ep1 (1994-1996), Ep2 (2000-2002) and Ep3 (2013-2015) are
463 clearly identified as major drought events that have been reported in previous studies (Min et
464 al. 2003; Kwon et al. 2016; Nam et al. 2015). As for Ep3, the amount of rainfall for this
465 period was less than 35-50% of the annual mean rainfall (1973-2015) and the estimated
466 return period was about 26 years (Kwon et al. 2016). Local governments during this dry
467 period implemented a plan to restrict water usage in many cities across South Korea, thus
468 confirming that the MSDI can accurately reproduce the historical drought.
469 **[Figs. 13-14; Tab. 4]**
470
471 **5. Concluding remarks**
472 Drought is an increasingly important issue in many parts of the world, requiring a hydro-
473 meteorological modeling framework to assess and monitor its complex impact on natural
474 hazards and associated socio-economic vulnerability. Here, we use two representative
475 drought indices (the SPI and SSI) to evaluate changes in drought patterns at different spatio-
476 temporal scales. The SPI and SSI, derived from precipitation and SM, respectively, are
477 compared with each other by describing their individual characteristics as drought indicators
478 as well as their interdependence and interaction. Furthermore, considering different aspects of
479 the drought dynamics, this study introduces the MSDI, which is used to consider
480 meteorological and agricultural droughts jointly in the context of a multivariate probability
481 distribution. The MSDI derived for each station is then grouped using the hierarchical

clustering approach for better understanding of the regional features of drought conditions. The primary conclusions obtained in this study are as follows:

1. The transition from meteorological to agricultural drought is clearly identified, but the degree of their relationship is significantly dependent on the season. Specifically, the SSI had a 1-month delayed response to the SPI during the dry season (i.e., winter-spring), whereas the response of the SSI to SPI is generally prompt under wet soil conditions. Thus, one should consider the role of antecedent SM content to improve characterization of changes in drought propagation.
2. The SSI shows less frequent droughts and longer drought duration, due to the gradual decrease in the autocorrelation functions of SSI along with the higher degree of autocorrelation, compared to that of the SPI. In this perspective, the onset of a drought could be detected by the SPI, whereas the SSI appears to be more appropriate for describing drought persistence. Overall, this is also supported by the fact that the 1-month lag between the SPI and SSI was significant for most stations over the last three decades (1986-2016).
3. In this study, the copula-based MSDI is employed to consider the interdependence and interaction between rainfall and SM in the context of a multivariate probability distribution. Moreover, the hierarchical agglomerative clustering approach is employed to identify the spatial pattern of the MSDI. The distribution of the resulting clusters is contiguous rather than spatially isolated for both accumulation periods, contributing to more effective strategies in the development and implementation of drought management and mitigation plans for certain areas.
4. Here, we use a hierarchical clustering approach to the MSDI to investigate regional trends in drought pattern. By using this approach, the spatio-temporal drought patterns are clearly captured through the MSDI. Specifically, more drought episodes under

moderate to severe drought conditions are dominantly observed along the southern coast of South Korea. We also find persistent drought with a higher level of severity in the northern part of South Korea, which might be attributable to the significant decreasing trend (or increasing drought risk) that is noted in the northern part of South Korea. Overall, for a longer-duration MSDI-6, a significant downward trend has become more dominant.

Given that a drought index more effectively provides the status of drought for decision making in near-real time compared to raw data, and that a single drought index may not be sufficient for describing the complex aspects of drought, the findings and approaches used in this study are expected to provide useful guidelines for detecting the nature of droughts and contributing to drought preparedness. However, integration with other relevant drought indicators (e.g., streamflow and ground water) is still needed for a better understanding of multi-dimensional aspects of drought in future studies. Moreover, future work will also focus on the extension of data records with multiple sources such as satellite remote sensing data and multiple hydro-meteorological variables as potential predictors.



## Acknowledgments

The first author gratefully acknowledges the financial support provided by Korea Water Resources Corporation (K-water) for carrying out his PhD study at the University of Bristol. This work was also funded by the Korea Meteorological Administration Research and Development Program under Grant KMI 2018-07010.

## References

Agha Kouchak, A. 2015. A multivariate approach for persistence-based drought prediction: Application to the 2010-2011 East Africa drought. *Journal of Hydrology*, **526**: 127-135. doi: 10.1016/j.jhydrol.2014.09.063

Akaike, H. 1974. A New Look at the Statistical Model Identification. *IEEE Transactions on Automatic Control*, **19(6)**: 716-723.

Albergel, C. et al. 2012. Soil Moisture Analyses at ECMWF: Evaluation Using Global Ground-Based In Situ Observations. *Journal of Hydrometeorology*, **13(5)**: pp.1442-1460. *http://journals.ametsoc.org/doi/abs/10.1175/JHM-D-11-0107.1*

Bouyé, E. et al. 2000. Copulas for Finance - A Reading Guide and Some Applications. *SSRN Electronic Journal*. *http://www.ssrn.com/abstract=1032533*

Clayton, D. G. 1978. A Model for Association in Bivariate Life Tables and Its Application in Epidemiological Studies of Familial Tendency in Chronic Disease Incidence. *Biometrika*, **65(1)**: 141-151.

Dai, A. 2011. Drought under global warming: A review. *Wiley Interdisciplinary Reviews: Climate Change*, **2(1)**: 45-65.

Djerbouai, S. & Souag-Gamane, D. 2016. Drought Forecasting Using Neural Networks, Wavelet Neural Networks, and Stochastic Models: Case of the Algerois Basin in North Algeria. *Water Resources Management*, **30(7)**: 2445-2464.

Dracup, J. A., Lee, K. S. & Paulson, E. G., 1980. On the definition of droughts. *Water Resources Research*, **16(2)**: 297-302.

Ekanayake, E. & Perera, K. 2014. Analysis of Drought Severity and Duration Using Copulas in Anuradhapura, Sri Lanka. *British Journal of Environment and Climate Change*, **4(3)**: 312-327. *http://www.sciencedomain.org/abstract.php?iid=631&id=10&aid=6867*

Entekhabi, D., Rodriguez-Iturbe, I. & Castelli, F., 1996. Mutual interaction of soil moisture state and atmospheric processes. *Journal of Hydrology*, **184(1-2)**: 3-17.

Farahmand, A. & Agha Kouchak, A. 2015. A generalized framework for deriving nonparametric standardized drought indicators. *Advances in Water Resources*, **76**: 140-145. doi: 10.1016/j.advwatres.2014.11.012

Favre, A. C. et al. 2004. Multivariate hydrological frequency analysis using copulas. *Water Resources Research*, **40(1)**: 1-12.

Ganguli, P. & Ganguly, A. R. 2016. Space-time trends in U.S. meteorological droughts. *Journal of Hydrology: Regional Studies*, **8**: 235-259. doi: 10.1016/j.ejrh.2016.09.004

Güner Bacanli, Ü. 2017. Trend analysis of precipitation and drought in the Aegean region, Turkey. *Meteorological Applications*, **24(2)**: 239-249.

565 Guttman, N. B. 1999. Accepting the Standardized Precipitation Index: a Calculation
566 Algorithm1. *JAWRA Journal of the American Water Resources Association*, **35(2)**:
567 311-322.
568 Hao, Z. & AghaKouchak, A. 2013. Multivariate Standardized Drought Index: A parametric
569 multi-index model. *Advances in Water Resources*, **57**: 12-18. doi:
570 10.1016/j.advwatres.2013.03.009
571 Hao, Z. & Singh, V. P. 2015. Drought characterization from a multivariate perspective: A
572 review. *Journal of Hydrology*, **527**: 6680678. doi: 10.1016/j.jhydrol.2015.05.031
573 Hayes, M. et al. 2011. The lincoln declaration on drought indices: Universal meteorological
574 drought index recommended. *Bulletin of the American Meteorological Society*, **92(4)**:
575 485-488.
576 Joe, H., 1997. *NoMultivariate Models and Multivariate Dependence Concepts*, New York:
577 Chapman and Hall.
578 Jongman, B. et al. 2014. Increasing stress on disaster-risk finance due to large floods. *Nature*
579 *Climate Change*, **4(4)**: 264-268.
580 Kao, S. C. & Govindaraju, R. S., 2010. A copula-based joint deficit index for droughts.
581 *Journal of Hydrology*, 380(1-2): 121-134. doi: 10.1016/j.jhydrol.2009.10.029
582 Kim, B. J. et al. 2002. Summer monsoon rainfall patterns over South Korea and associated
583 circulation features. *Theoretical and Applied Climatology*, **72(1-2)**: 65-74.
584 Koenker, R. & Bassett, G. 1978. Regression quantiles. *Econometrica*, **46(1)**: 33-50.
585 Kumar, R. et al. 2016. Multiscale evaluation of the Standardized Precipitation Index as a
586 groundwater drought indicator. *Hydrology and Earth System Sciences*, **20(3)**: 1117-
587 1131.
588 Kwon, H. H., Lall, U. & Kim, S. J. 2016. The unusual 2013-2015 drought in South Korea in
589 the context of a multicentury precipitation record: Inferences from a nonstationary,
590 multivariate, Bayesian copula model. *Geophysical Research Letters*, **43(16):** 8534-
591 8544.
592 Lall, U., Devineni, N. & Kaheil, Y. 2016. An Empirical, Nonparametric Simulator for
593 Multivariate Random Variables with Differing Marginal Densities and Nonlinear
594 Dependence with Hydroclimatic Applications. *Risk Analysis*, **36(1)**: 57-73.
595 Li, C., Singh, V. P. & Mishra, A. K. 2013. A bivariate mixed distribution with a heavy-tailed
596 component and its application to single-site daily rainfall simulation. *Water Resources*
597 *Research*, **49(2)**: 767-789.

598 Li, X. et al. 2017. The East Asian summer monsoon variability over the last 145 years
599 inferred from the Shihua Cave record, North China. *Scientific Reports*, **7(1)**: 1-11. doi:
600 10.1038/s41598-017-07251-3
601 van Loon, A. F. et al. 2016. Drought in a human-modified world: Reframing drought
602 definitions, understanding, and analysis approaches. *Hydrology and Earth System*
603 *Sciences*, **20(9)**: 3631-3650.
604 van Loon, A. F. 2015. Hydrological drought explained. *Wiley Interdisciplinary Reviews:*
605 *Water*, **2(4)**: 359-392. doi: 10.1002/wat2.1085
606 Martinez, W. L. & Martinez, A. R. 2004. *Exploratory Data Analysis with MATLAB*. doi:
607 10.1201/9780203483374
608 Mckee, T. B., Doesken, N. J. & Kleist, J. 1993. The relationship of drought frequency and
609 duration to time scales. *AMS 8th Conference on Applied Climatology*, (January), 179-
610 184. *http://ccc.atmos.colostate.edu/relationshipofdroughtfrequency.pdf*
611 Meng, L., Ford, T. & Guo, Y. 2017. Logistic regression analysis of drought persistence in
612 East China. *International Journal of Climatology*, **37(3)**: 1444-1455.
613 Min, S. K. et al. 2003. Spatial and temporal comparisons of droughts over Korea with East
614 Asia. *International Journal of Climatology*, **23(2)**: 223-233.
615 Mirabbasi, R. et al. 2013. Analysis of meteorological drought in northwest Iran using the
616 Joint Deficit Index. *Journal of Hydrology*, **492**: 35-48. doi:
617 10.1016/j.jhydrol.2013.04.019
618 Mirabbasi, R., Fakheri-Fard, A. & Dinpashoh, Y. 2012. Bivariate drought frequency analysis
619 using the copula method. *Theoretical and Applied Climatology*, **108(1-2)**: 191-206.
620 Mo, K. C. 2011. Drought onset and recovery over the United States. *Journal of Geophysical*
621 *Research Atmospheres*, **116(20)**: 1-14.
622 Mojena, R., 1977. Hierarchical grouping methods and stopping rules: An evaluation. *Coputer*
623 *Journal*, 20 (April), 359-363.
624 Nam, W. H. et al. 2015. Drought hazard assessment in the context of climate change for
625 South Korea. *Agricultural Water Management*, **160**: 106-117. doi:
626 10.1016/j.agwat.2015.06.029
627 Narasimhan, B. & Srinivasan, R. 2005. Development and evaluation of Soil Moisture Deficit
628 Index (SMDI) and Evapotranspiration Deficit Index (ETDI) for agricultural drought
629 monitoring. *Agricultural and Forest Meteorology*, **133(1-4)**: 69-88.
630 Nelsen, R. B. 1999. An Introduction to Copulas. In New York: Springer.

631 Palmer, W. C. 1965. Meteorological Drought. *U.S. Weather Bureau, Res. Pap. No. 45*, 58.
632 *https://www.ncdc.noaa.gov/temp-and-precip/drought/docs/palmer.pdf*
633 Pebesma, E. J., 2004. Multivariable geostatistics in S: The gstat package. *Computers and*
634 *Geosciences*, **30(7)**: 683-691.
635 Renard, B. & Lang, M. 2007. Use of a Gaussian copula for multivariate extreme value
636 analysis: Some case studies in hydrology. *Advances in Water Resources*, **30(4)**: 897-
637 912.
638 Requena, A. I., Mediero, L. & Garrote, L. 2013. A bivariate return period based on copulas
639 for hydrologic dam design: Accounting for reservoir routing in risk estimation.
640 *Hydrology and Earth System Sciences*, **17(8)**: 3023-3038.
641 Rüschendorf, L. 2009. On the distributional transform, Sklar's theorem, and the empirical
642 copula process. *Journal of Statistical Planning and Inference*, **139(11)**: 3921-3927.
643 Salvadori, G. & de Michele, C. 2004. Frequency analysis via copulas: Theoretical aspects and
644 applications to hydrological events. *Water Resources Research*, **40(12)**: 1-17.
645 Santos, J. F., Pulido-Calvo, I. & Portela, M. M. 2010. Spatial and temporal variability of
646 droughts in Portugal. *Water Resources Research*, **46(3)**: 1-13.
647 Shafer, B. A. & Dezman, L. E., 1982. Development of a surface water supply index (SWSI)
648 to assess the severity of drought conditions in snowpack runoff areas. *Western Snow*
649 *Conference*, 164-175.
650 Shamshirband, S. et al. 2015. Clustering project management for drought regions
651 determination: A case study in Serbia. *Agricultural and Forest Meteorology*, **200**: 57-
652 65.
653 Shiau, J. T. & Lin, J. W., 2016. Clustering Quantile Regression-Based Drought Trends in
654 Taiwan. *Water Resources Management*, **30(3)**: 1053-1069.
655 Shukla, S., Steinemann, A. C. & Lettenmaier, D. P. 2011. Drought Monitoring for
656 Washington State: Indicators and Applications. *Journal of Hydrometeorology*, **12(1)**:
657 66-83. doi: 10.1175/2010JHM1307.1
658 Sklar, M., 1959. Fonctions de Répartition À N Dimensions Et Leurs Marges. In Publications
659 de l'Institut de Statistique de L'Université de Paris 8, 229-231.
660 Spinoni, J. et al. 2014. World drought frequency, duration, and severity for 1951-2010.
661 *International Journal of Climatology*, **34(8)**: 2792-2804.
662 Sprenger, M. et al., 2016. A copula-based nonstationary frequency analysis for the 2012-2015
663 drought in California. *Water Resources Research*, **52**: 5727-5754.

664 Subash, N. & Ram Mohan, H. S. 2011. Trend detection in rainfall and evaluation of
665 standardized precipitation index as a drought assessment index for rice-wheat
666 productivity over IGR in India. *International Journal of Climatology*, 31(11), 1694-
667 1709.
668 Svoboda, M. D. & Fuchs, B. A. 2017. *Handbook of drought indicators and indices*.
669 Tatli, H. 2015. Detecting persistence of meteorological drought via the Hurst exponent.
670 *Meteorological Applications*, **22(4)**: 763-769.
671 Vicente-Serrano, S. M., Beguería, S. & López-Moreno, J. I. 2010. A multiscalar drought
672 index sensitive to global warming: The standardized precipitation evapotranspiration
673 index. *Journal of Climate*, **23(7)**: 1696-1718.
674 Vidal, J.-P. et al. 2009. Multilevel and multiscale drought reanalysis over France with the
675 Safran-Isba-Modcou hydrometeorological suite. *Hydrology and Earth System*
676 *Sciences Discussions*, **6(5)**: 6455-6501. *http://www.hydrol-earth-syst-sci-*
677 *discuss.net/6/6455/2009/*
678 Yang, P. et al. 2017. Quantile regression and clustering analysis of standardized precipitation
679 index in the Tarim River Basin, Xinjiang, China. *Theoretical and Applied*
680 *Climatology*.
681 Yoo, J. et al. 2012. Drought frequency analysis using cluster analysis and bivariate
682 probability distribution. *Journal of Hydrology*, **420-421**: 102-111. doi:
683 10.1016/j.jhydrol.2011.11.046
684 Zargar, A. et al., 2011. A review of drought indices. *Environmental Reviews*, **19(NA)**: 333-
685 349. doi: /10.1139/a11-013
686 Zhang, L. & Singh, V. P. 2006. Bivariate Flood Frequency Analysis Using the Copula
687 Method. *Water*, 11 (April): 150-164.
688 Zhang, L. & Zhou, T., 2015. Drought over East Asia: A review. *Journal of Climate*, 28(8):
689 3375-3399.

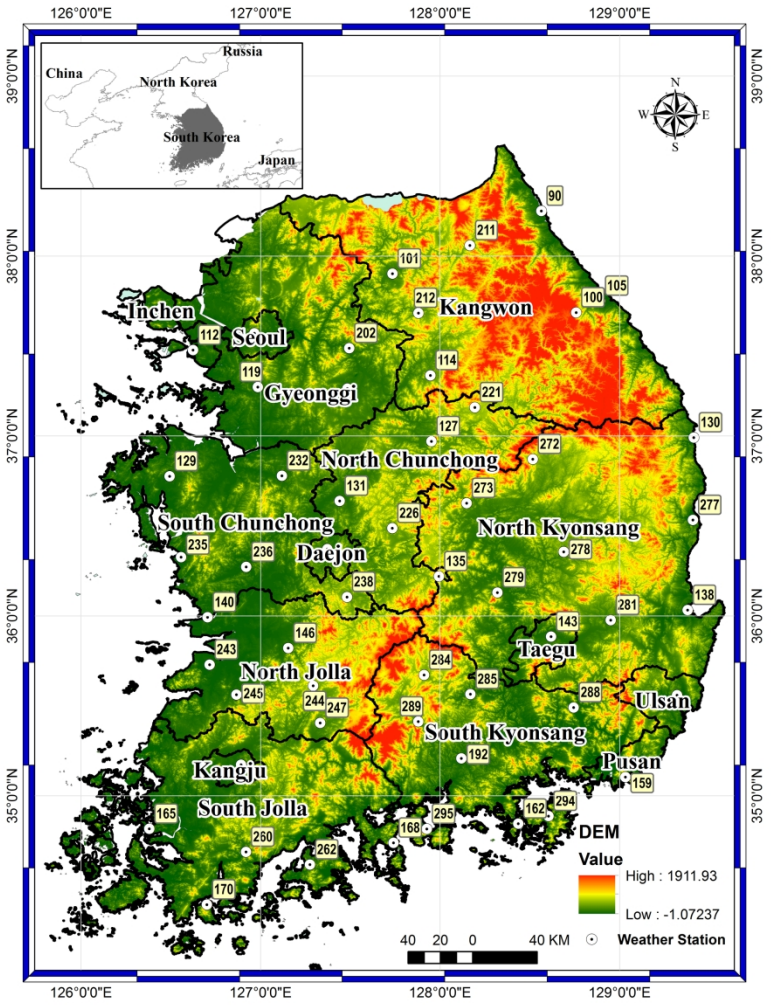


Figure 1. Topographic map showing the locations of weather stations used in this study. Here, black solid lines indicate province boundaries.

210x296mm (300 x 300 DPI)

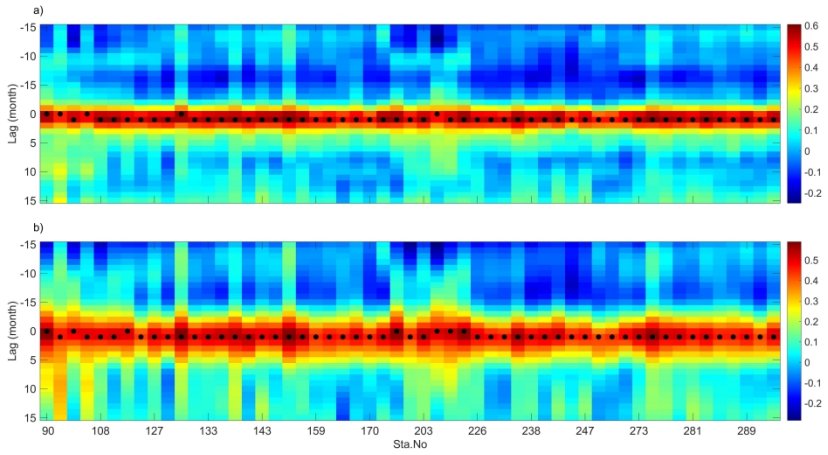


Figure 2. Heat maps showing cross-correlation coefficients between SPI and lagged SSI over the entire array of weather stations. Here, a) and b) represent accumulation periods of 3 and 6 months, respectively.

508x266mm (300 x 300 DPI)

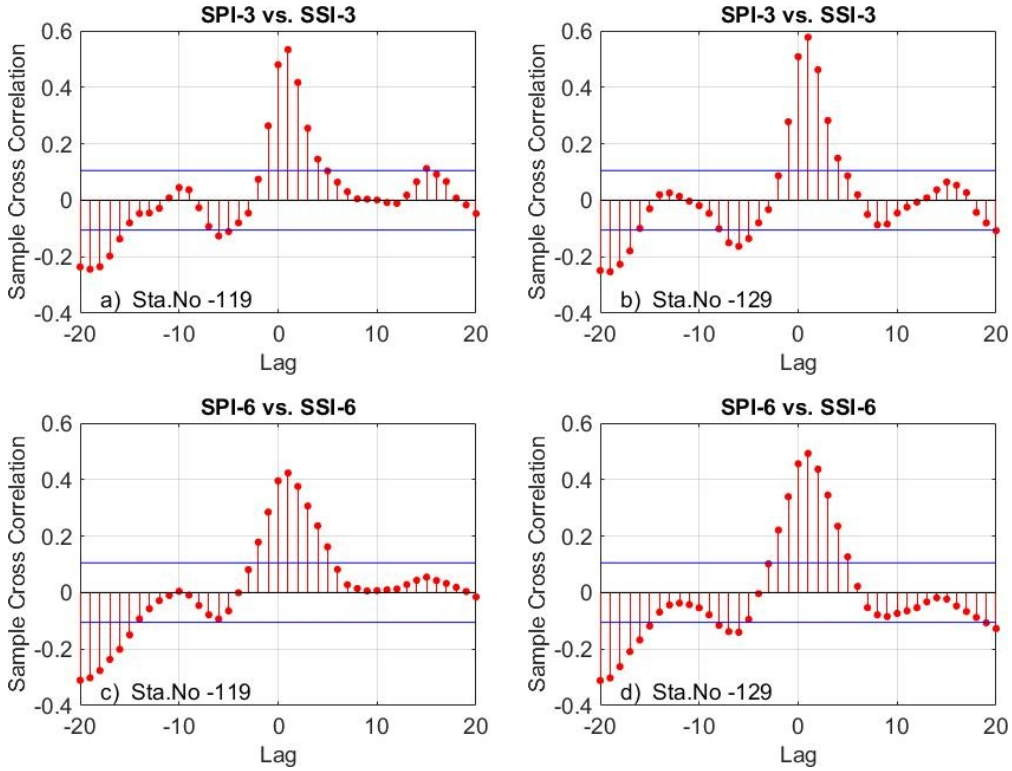


Figure 3. Samples of cross-correlation between SPI and SSI for 3- and 6-month time scale.

71x54mm (300 x 300 DPI)

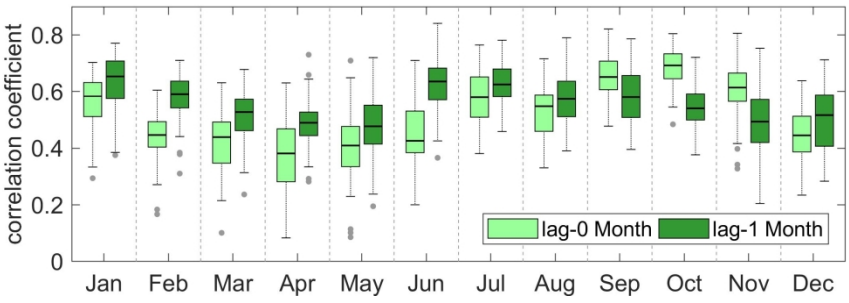


Figure 4. Boxplots of the Pearson correlation coefficients for identifying time-lagged relationships between the SPI-3 and SSI-3 time series on a monthly basis across all stations.

211x66mm (300 x 300 DPI)

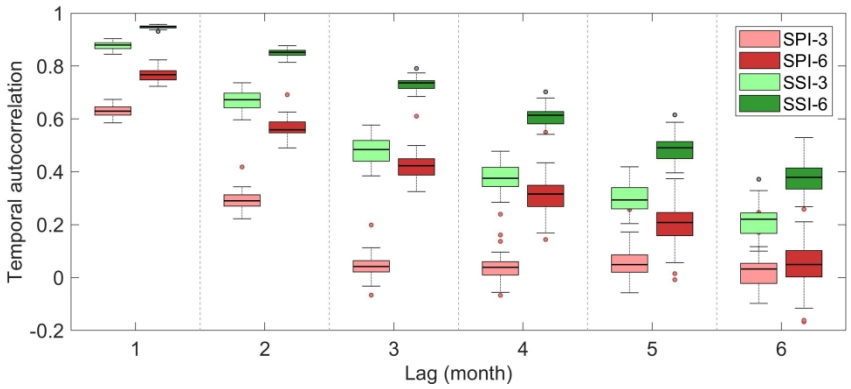


Figure 5. Temporal autocorrelation functions of SPIs and SSIs representing drought persistence with respect to different time lags.

264x105mm (300 x 300 DPI)

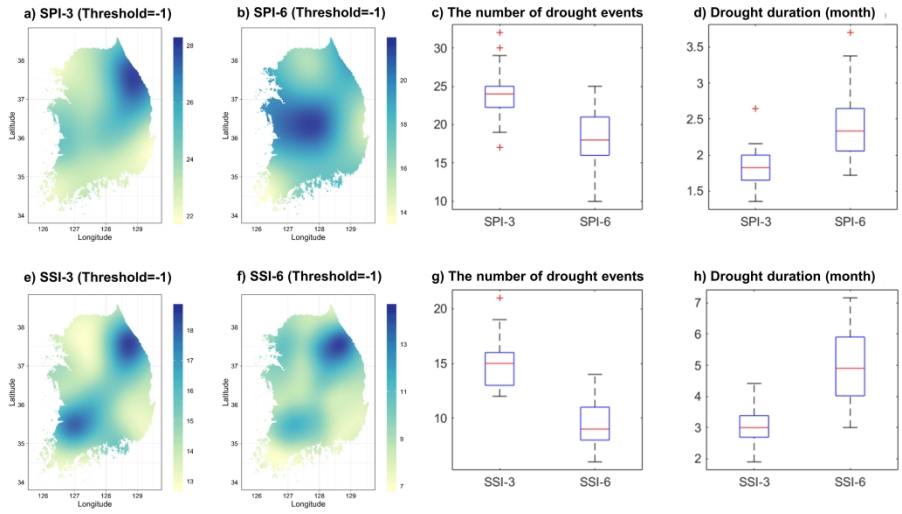


Figure 6. Characteristics of SPI/SSI-n drought events based on a threshold of -1.0 (moderate drought): a-b and e-f show the spatial distributions of drought events across South Korea along with their boxplots (c and g), and their corresponding average drought durations are presented in d and h.

338x190mm (300 x 300 DPI)

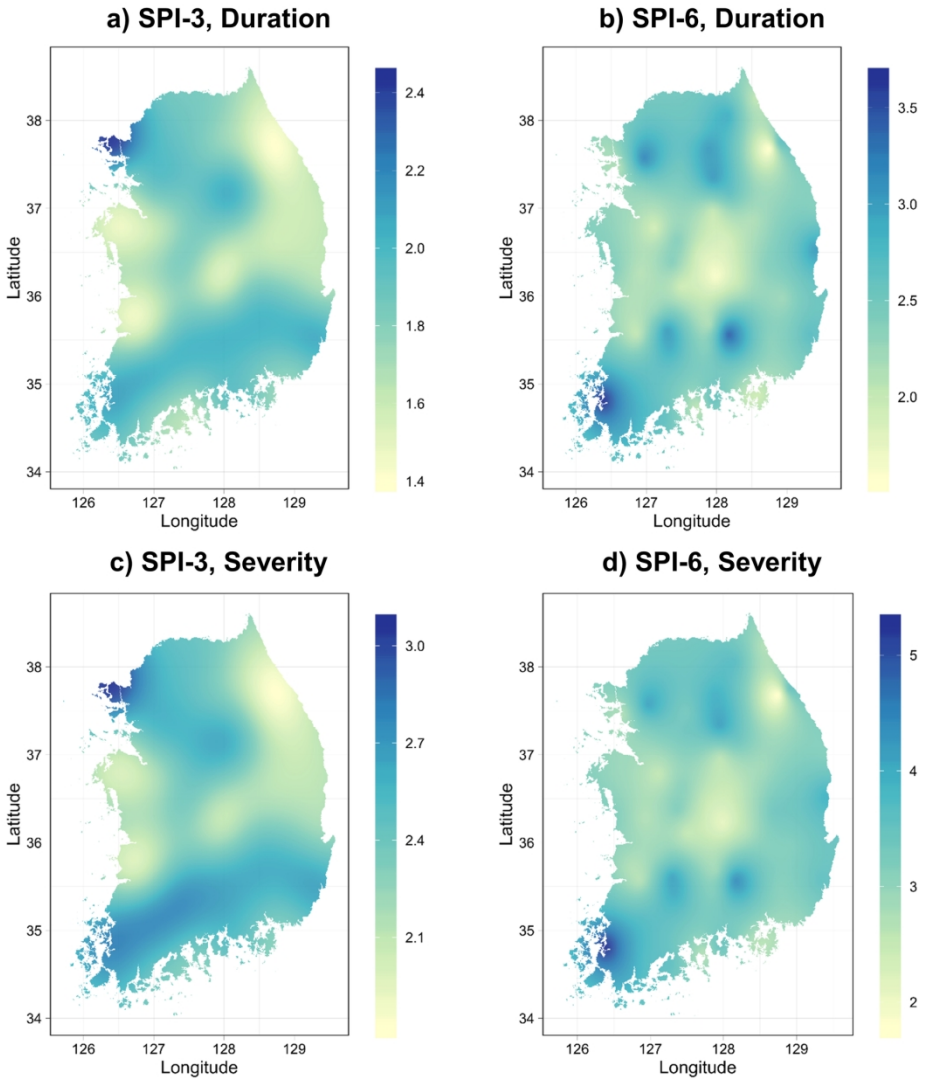


Figure 7. Spatial distribution patterns of meteorological drought (SPI-n) duration and severity using a threshold of -1.0 (moderate drought).

170x189mm (300 x 300 DPI)

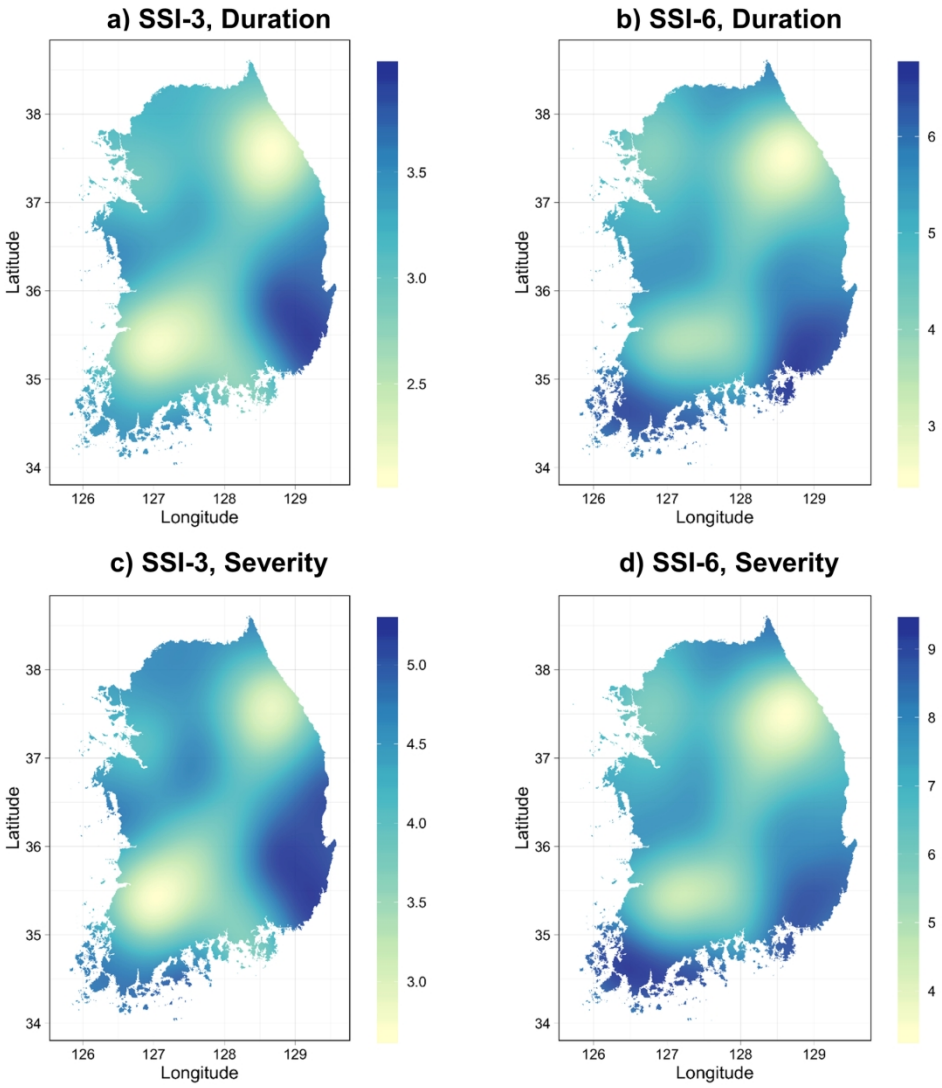


Figure 8. Spatial distribution patterns of agricultural drought (SSI-n) duration and severity using a threshold of -1.0 (moderate drought).

170x189mm (300 x 300 DPI)

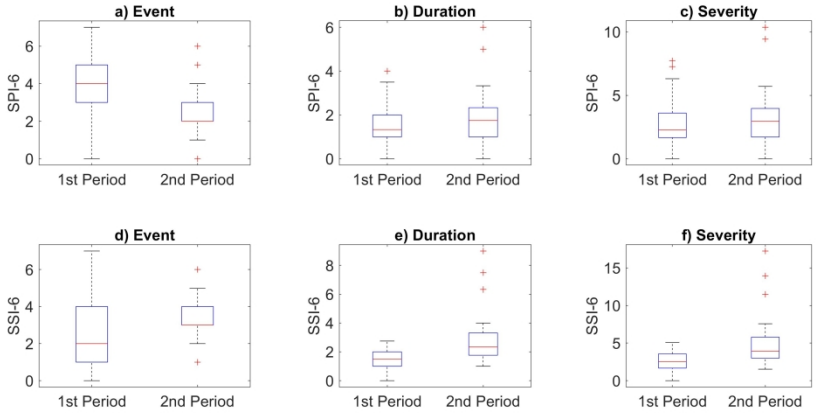


Figure 9. Comparison of drought variables (i.e. frequency, duration and severity) between the first half (1987-2001) and second half (2002-2016) of the period 1987-2016.

344x158mm (300 x 300 DPI)

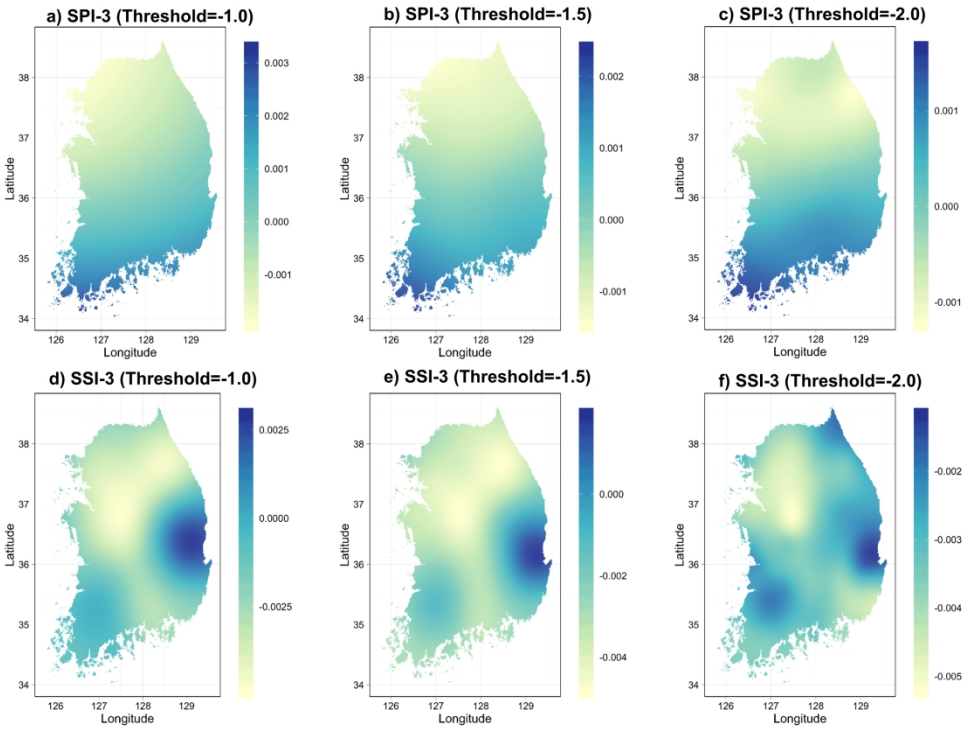


Figure 10. Spatial distribution of trends in SPI-6 and SSI-6 at different quantile levels.

260x190mm (300 x 300 DPI)

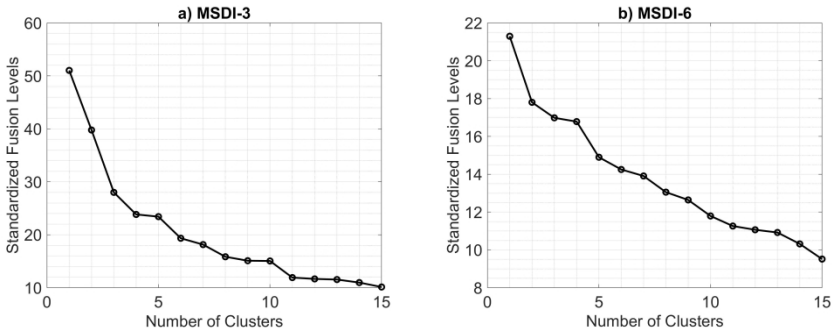


Figure 11. Standardized fusion levels corresponding to the number of clusters for MSDI-3 and MSDI-6.

396x132mm (300 x 300 DPI)

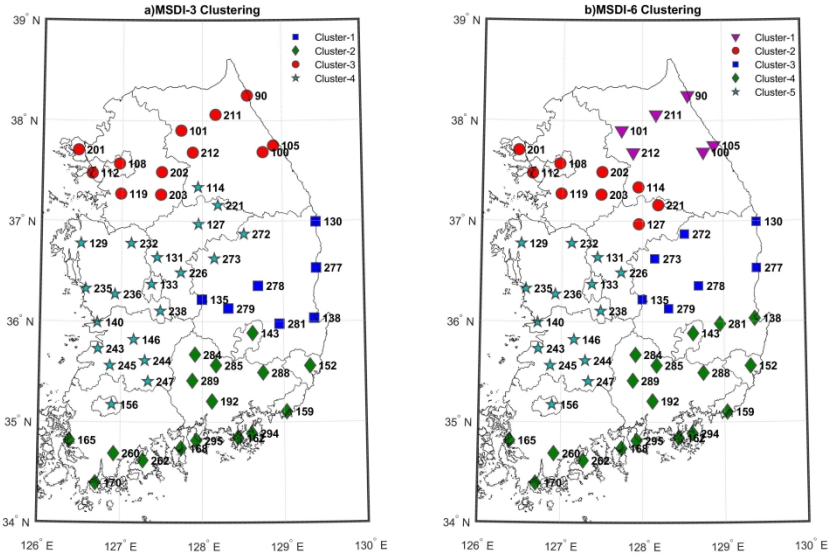


Figure 12. Spatial distribution of clusters for the MSDI over South Korea. Left panel, MSDI-3; right panel, MSDI-6.

317x211mm (300 x 300 DPI)

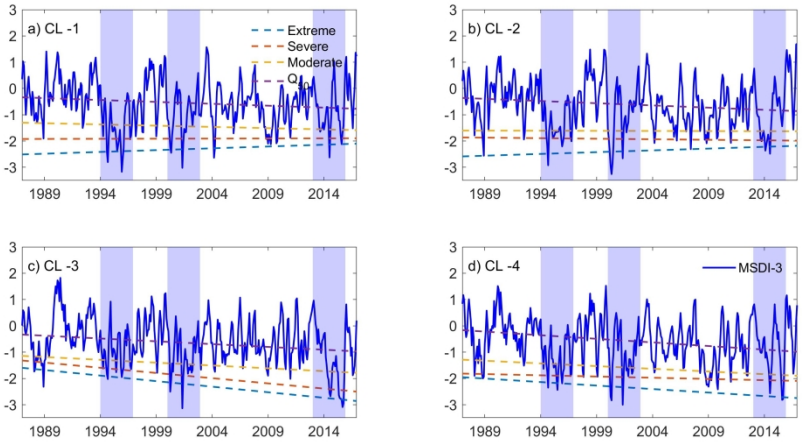


Figure 13. Regional trends of MSDI-3 corresponding to each cluster and their trends over different thresholds based on a quantile regression. Here, blue bars denote three major drought episodes over the past three decades.

317x158mm (300 x 300 DPI)

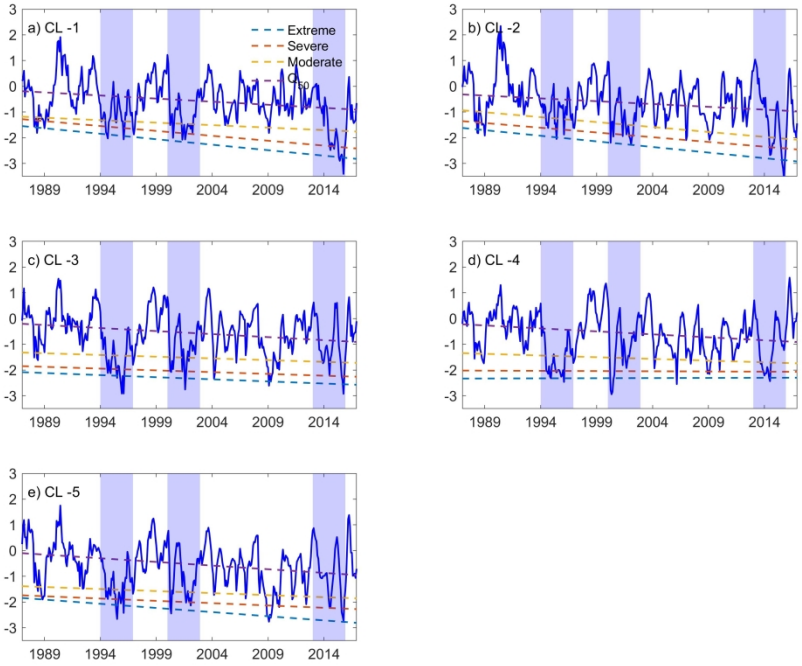


Figure 14. Regional trends of MSDI-6 corresponding to each cluster and their trends over different thresholds based on a quantile regression. Here, blue bars denote three major drought episodes over the past three decades.

317x246mm (300 x 300 DPI)

Table 1. Rainfall stations used in this study and their annual rainfall.

| Sta. No | Sta. Name | Lat. (N) | Lon. (E) | Alt. (m) | Rainfall (mm) | | | | | Sta. No | Sta. Name | Lat. (N) | Lon. (E) | Alt. (m) | Rainfall (mm) | | | | |
|---|---|---|---|---|---|---|---|---|---|---|---|---|---|---|---|---|---|---|---|
| | | | | | Annual | NDJ | FMA | MJJ | ASO | | | | | | Annual | NDJ | FMA | MJJ | ASO |
| 90 | Sokcho | 38.25 | 128.56 | 18.1 | 1,386 | 142 | 207 | 653 | 384 | 203 | Icheon | 37.26 | 127.48 | 78.0 | 1,277 | 109 | 273 | 631 | 264 |
| 100 | Daegwallyeong | 37.69 | 128.76 | 772.6 | 1,765 | 150 | 274 | 897 | 444 | 211 | Inje | 38.06 | 128.17 | 200.2 | 1,394 | 120 | 241 | 786 | 247 |
| 101 | Chuncheon | 37.90 | 127.74 | 76.5 | 1,356 | 70 | 205 | 850 | 231 | 212 | Hongcheon | 37.68 | 127.88 | 140.0 | 1,520 | 119 | 383 | 757 | 262 |
| 105 | Gangneung | 37.75 | 128.89 | 26.0 | 1,451 | 154 | 222 | 653 | 422 | 221 | Jecheon | 37.16 | 128.19 | 259.8 | 1,463 | 113 | 384 | 705 | 260 |
| 108 | Seoul | 37.57 | 126.97 | 85.8 | 1,453 | 69 | 214 | 919 | 251 | 226 | Boeun | 36.49 | 127.73 | 175.0 | 1,163 | 110 | 231 | 595 | 228 |
| 112 | Incheon | 37.48 | 126.62 | 68.2 | 1,237 | 64 | 194 | 742 | 238 | 232 | Cheonan | 36.78 | 127.12 | 81.5 | 1,445 | 96 | 351 | 750 | 248 |
| 114 | Wonju | 37.34 | 127.95 | 148.6 | 1,346 | 73 | 203 | 819 | 252 | 235 | Boryeong | 36.33 | 126.56 | 15.5 | 1,536 | 127 | 384 | 737 | 288 |
| 119 | Suwon | 37.27 | 126.99 | 34.1 | 1,327 | 73 | 207 | 803 | 244 | 236 | Buyeo | 36.27 | 126.92 | 11.3 | 1,524 | 107 | 340 | 803 | 274 |
| 127 | Chungju | 36.97 | 127.95 | 116.3 | 1,239 | 75 | 199 | 721 | 244 | 238 | Geumsan | 36.11 | 127.48 | 170.4 | 1,337 | 58 | 210 | 818 | 251 |
| 129 | Seosan | 36.78 | 126.49 | 28.9 | 1,273 | 91 | 219 | 714 | 249 | 243 | Buan | 35.73 | 126.72 | 12.0 | 1,409 | 68 | 202 | 893 | 246 |
| 130 | Uljin | 36.99 | 129.41 | 50.0 | 1,155 | 133 | 197 | 508 | 318 | 244 | Imsil | 35.61 | 127.29 | 247.9 | 1,361 | 74 | 215 | 810 | 263 |
| 131 | Cheongju | 36.64 | 127.44 | 58.7 | 1,242 | 83 | 203 | 717 | 240 | 245 | Jeongeup | 35.56 | 126.87 | 69.8 | 1,197 | 60 | 189 | 729 | 218 |
| 133 | Daejeon | 36.37 | 127.37 | 68.9 | 1,366 | 97 | 225 | 792 | 252 | 247 | Namwon | 35.41 | 127.33 | 132.5 | 1,362 | 65 | 209 | 843 | 245 |
| 135 | Chupungnyeong | 36.22 | 127.99 | 243.7 | 1,897 | 136 | 484 | 931 | 346 | 260 | Jangheung | 34.69 | 126.92 | 45.0 | 1,412 | 82 | 231 | 847 | 253 |
| 138 | Pohang | 36.03 | 129.38 | 2.3 | 1,850 | 144 | 479 | 906 | 322 | 262 | Goheung | 34.62 | 127.28 | 53.1 | 1,308 | 89 | 219 | 767 | 233 |
| 140 | Gunsan | 35.99 | 126.71 | 23.2 | 1,554 | 97 | 282 | 873 | 302 | 272 | Yeongju | 36.87 | 128.52 | 210.8 | 1,238 | 78 | 191 | 718 | 251 |
| 143 | Daegu | 35.89 | 128.62 | 53.5 | 1,233 | 80 | 258 | 673 | 222 | 273 | Mungyeong | 36.63 | 128.15 | 170.6 | 1,230 | 93 | 203 | 690 | 244 |
| 146 | Jeonju | 35.82 | 127.15 | 61.4 | 1,298 | 77 | 236 | 747 | 237 | 277 | Yeongdeok | 36.53 | 129.41 | 42.1 | 1,358 | 97 | 235 | 773 | 254 |
| 152 | Ulsan | 35.56 | 129.32 | 83.2 | 1,309 | 88 | 230 | 744 | 247 | 278 | Uiseong | 36.36 | 128.69 | 81.8 | 1,289 | 98 | 220 | 746 | 225 |
| 156 | Gwangju | 35.17 | 126.89 | 72.4 | 1,091 | 68 | 199 | 604 | 220 | 279 | Gumi | 36.13 | 128.32 | 48.9 | 1,222 | 113 | 211 | 661 | 237 |
| 159 | Busan | 35.10 | 129.03 | 69.6 | 1,073 | 69 | 210 | 589 | 205 | 281 | Yeongcheon | 35.98 | 128.95 | 93.8 | 1,352 | 107 | 226 | 774 | 244 |
| 162 | Tongyeong | 34.85 | 128.44 | 32.3 | 1,078 | 107 | 202 | 505 | 263 | 284 | Geochang | 35.67 | 127.91 | 226.0 | 1,327 | 124 | 226 | 722 | 254 |
| 165 | Mokpo | 34.82 | 126.38 | 38.0 | 1,015 | 59 | 189 | 576 | 191 | 285 | Hapcheon | 35.57 | 128.17 | 32.0 | 1,348 | 103 | 229 | 772 | 243 |
| 168 | Yeosu | 34.74 | 127.74 | 64.6 | 1,185 | 86 | 210 | 668 | 221 | 288 | Miryang | 35.49 | 128.74 | 11.2 | 1,485 | 106 | 310 | 804 | 265 |
| 170 | Wando | 34.40 | 126.70 | 35.2 | 1,183 | 115 | 227 | 562 | 279 | 289 | Sancheong | 35.41 | 127.88 | 138.1 | 1,448 | 103 | 355 | 735 | 254 |
| 192 | Jinju | 35.21 | 128.12 | 30.2 | 1,243 | 105 | 211 | 688 | 240 | 294 | Geoje | 34.89 | 128.60 | 45.4 | 1,322 | 75 | 255 | 748 | 244 |
| 201 | Ganghwa | 37.71 | 126.45 | 47.0 | 1,075 | 68 | 200 | 597 | 210 | 295 | Namhae | 34.82 | 127.93 | 43.7 | 1,288 | 77 | 241 | 742 | 230 |
| 202 | Yangpyeong | 37.49 | 127.49 | 48.0 | 1,293 | 105 | 218 | 740 | 231 | | | | | | | | | | |

Table 2. The SPI (SSI) drought severity classification and interpretation.

| **SPI values** | **Drought category** |
|---|---|
| ≥ 2.0 | Extremely wet |
| 1.5 to 1.99 | Severely wet |
| 1.0 to 1.49 | Moderately wet |
| 0.99 to -0.99 | Near normal |
| -1.0 to -1.49 | Moderately dry |
| -1.5 to -1.99 | Severely dry |
| ≤ -2.0 | Extremely dry |

Table 3. Summary of drought episodes based on clustering analysis.

| Threshold | Number of Events | | | | | Duration | | | | | Severity | | | | |
|---|---|---|---|---|---|---|---|---|---|---|---|---|---|---|---|
| | CL-1 | CL-2 | CL-3 | CL-4 | CL-5 | CL-1 | CL-2 | CL-3 | CL-4 | CL-5 | CL-1 | CL-2 | CL-3 | CL-4 | CL-5 |
| **MSDI-3** | | | | | | | | | | | | | | | |
| Moderate | 33 | 29 | **41** | 34 | | 3.4 | **4.5** | 3.0 | 3.5 | | 5.5 | **7.2** | 4.6 | 5.6 | |
| Severe | 22 | 25 | **26** | **26** | | 2.6 | **2.8** | 2.2 | 2.5 | | 5.1 | **5.4** | 4.2 | 4.8 | |
| Extreme | 11 | **13** | 7 | 11 | | 1.8 | 1.6 | **2.3** | 1.6 | | 4.4 | 3.8 | **5.8** | 3.9 | |
| **MSDI-6** | | | | | | | | | | | | | | | |
| Moderate | **25** | **25** | 23 | 20 | 24 | 4.6 | 4.8 | 5.2 | **6.4** | 5.0 | 7.1 | 7.6 | 8.3 | **10.3** | 8.2 |
| Severe | 17 | **20** | 16 | 17 | 19 | 2.6 | 2.7 | **3.9** | 3.8 | 3.8 | 5.4 | 5.3 | **7.6** | 7.4 | 7.4 |
| Extreme | 7 | 7 | **11** | 9 | 12 | 3.1 | 2.7 | 2.3 | **3.3** | 2.0 | 7.5 | 6.6 | 5.3 | **7.5** | 4.7 |

Table 4. Summary of the slope obtained from a quantile regression model at four different classes. Numbers in bold are statistically significant at the 0.05 level.

| Cluster | MSDI-3 (× $10^{-3}$) | | | | MSDI-6 (× $10^{-3}$) | | | |
|---|---|---|---|---|---|---|---|---|
| | **Extreme** | **Severe** | **Moderate** | **$Q_{50}$** | **Extreme** | **Severe** | **Moderate** | **$Q_{50}$** |
| CL-1 | 1.14 | 0.07 | -0.79 | -1.21 | **-3.55** | **-3.17** | **-1.60** | **-2.00** |
| CL-2 | 1.13 | -0.34 | -0.07 | **-1.39** | **-3.63** | **-3.07** | **-3.19** | **-1.82** |
| CL-3 | **-3.51** | **-3.29** | **-1.79** | **-1.78** | -1.36 | -1.15 | -1.11 | **-1.96** |
| CL-4 | **-2.21** | -0.77 | **-1.70** | **-2.28** | 0.09 | -0.13 | -1.10 | **-1.92** |
| CL-5 | | | | | **-2.69** | -1.49 | -1.32 | **-2.37** |

# Spatio-temporal drought patterns of multiple drought indices based on precipitation and soil moisture: A case study in South Korea

**Moonhyuk Kwon, Hyun-Han Kwon* and Dawei Han**

We explore the spatio-temporal characteristics of meteorological and agricultural droughts, respectively, as well as their relationships over the past three decades (1986-2016). Further, the hierarchical agglomerative clustering approach is employed to identify the spatial pattern of the combined drought indices (the SSI and SPI) in South Korea.